Polymer Bulletin (2021) 78:6441–6454
https://doi.org/10.1007/s00289-020-03436-5

ORIGINAL PAPER

Superabsorbent composites (SACs) based on xanthan gum-*g*-poly (itaconic acid)/kaolinite

Preeti Sharma[1] · Anju Dagar[1] · Sapna[1] · Aparna Vyas[2] · Arpit Sand[1]

Received: 8 June 2020 / Revised: 7 September 2020 / Accepted: 18 October 2020 /
Published online: 26 October 2020

Abstract

In this present investigation, crosslinked polyitaconic acid (PIA) was grafted onto natural polysaccharides xanthan gum and inorganic clay kaolinite using free radical polymerization in an inert atmosphere using FTIR ammonium persulfate (APS) as an initiator and Tetra (ethylene glycol) diacrylate (TEGDA) as a crosslinking agent. Scanning electron microscopy and Fourier transform infrared spectra techniques were used to characterized for structure SAPs. The effect of various parameters which include APS, TEGDA, neutralizing degree, kaolinite contents, and xanthan gum was investigated. The results indicate that PIA successfully grafted onto xanthan gum and a 3D structure was formed. The results indicated with an increasing Xanthan gum/kaolin weight ratio, swelling capacity, and gel content.

Keywords Solution polymerization · Superabsorbent · Absorbency under load

Introduction

3D cross-linked hydrophilic polymer can absorb a huge capacity of water, salty solution, and retain the excess amount of water in a swollen state known as Superabsorbent Polymers. The above property arises due to the occurrence of various reactive sets such as hydroxyl, NH_2, and carboxylic attaching onto the polymeric backbone and do not separate even high temperature or pressure [1]. With the presence of excellent swelling ratio and outstanding hydrophilic property utility of superabsorbent polymers consider in a large spectrum of application such as drug delivery systems [2–4], farming and cultivation [5, 6], fastening mixtures

Electronic supplementary material The online version of this article (https://doi.org/10.1007/s00289-020-03436-5) contains supplementary material, which is available to authorized users.

✉ Arpit Sand
arpit@mru.edu.in

[1] Department of Chemistry, Manav Rachna University, Faridabad 121001, India

[2] Department of Mathematics, Manav Rachna University, Faridabad 121001, India

[7], biosensors [8, 9], non-natural snowfall [10], and boring runny flavors [11]. The absorbing property of superabsorbent polymers [12] composites applications improved by many methods. Inorganic materials such as Montmorillonite [13, 14], attapulgite [15, 16], kaolin [17, 18], mica [19, 20], bentonite, and sercite [21, 22] paid more consideration superabsorbent composites recently.

Hydroxyl groups present in the inorganic powders get hydrated aluminosilicates layered on the external surface. On the interaction between vinyl monomers, natural polymers (reactive sites), and mineral powders such as kaolinite results into a superabsorbent composite (SAPc). The use of mineral powders not only cuts manufacture prices but also advances the assets (such as enlargement ability thermal stability, gel strength and mechanical, etc.) of superabsorbent polymers and promptness up the generation of new materials for distinct solicitations [23, 24]. The SAPCs find many new applications beyond those of SAPS, such as nanocomposite materials, for example, fabrication of silver or zinc nanoparticles in SAP or SAPC networks. The proven applications are for catalysis, optics, electronics, bio-medicals, and quantum-sized domain applications. Some potential application of SAPCs in water treatments has been described. Several types of research on nanocomposites based on neodymium nitrate and rare earth zirconates dominated towards the investigation of photocatalytic behavior also studied [25–34].

Xanthan gum and crosslink with itaconic acid (IA) and kaolinite was dispersed in water. The structure of the Schematic diagram of kaolinite is represented in Scheme 1a. Superabsorbent polymer based on natural occurrence polysaccharides constitutes the majority of its formation due to remarkable properties, that is, nontoxicity, renewability, biocompatibility, and biodegradability. In the case of xanthan gum, extracellular anionic with molecular weight heteropolysaccharide acidic in nature with branched structure produced by Xanthomonas campestris (gram-negative bacterium) originates from cane sugar and derivatives of corn under aerobic circumstances [35, 36]. Although the distribution of side chains reflects average values, it is by evidence for repeat unit structure in microbial heteropolysaccharides and with the sharp temperature transition in optical rotation displayed by depyruvated xanthan gum as contrasted with the broad transition displayed by the native. Many properties of xanthan gum dispersion indicate that molecule assumes rod-like, ordered secondary structure. A sharp increase in the viscosity of 0.5–1.0% aqueous dispersions has been noted at 50–60 °C and confirmed by optical rotation, circular dichroism, and NMR measurements. Increasing the ionic strength raises the temperature at which the transition occurs, such melting out or denaturation is a helix-to-coil conformational transition, which is similar to that observed for double-stranded nucleic acids, triple-stranded collagen, and certain polysaccharide.

The structure of xanthan gum Scheme 1b is schematically represented. In this present paper, eco-friendly and low price superabsorbent composites centered on xanthan gum-graft-poly (itaconic acid)/kaolinite prepared with graft copolymerization as described in previous [37, 38] and it was found that 500 times water absorbency increased by weight. The effect of the kaolinite, crosslinker (TEGDA), and initiator (APS) as well as the polymerization method on the subsequent porous assets is deliberated. Absorbency under load (AUL) was also determined.

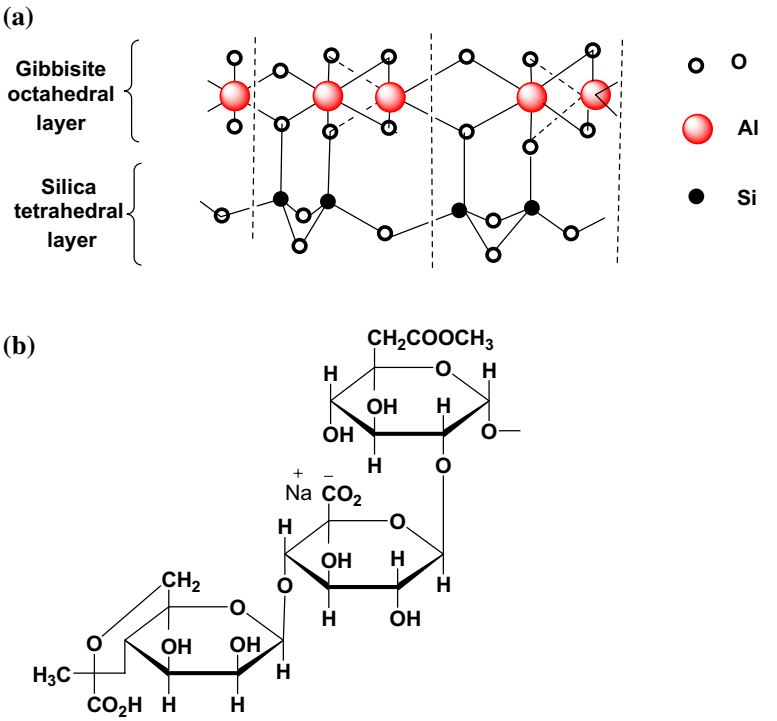

Scheme 1 Graphic arrangements of **a** Kaolinite, **b** structure of xanthan gum (XG)

Experimental

Materials

Itaconic acid (IA), Xanthan gum (XG Molecular weight 2000 kDa, intrinsic viscosity = 8.4 dl/g), Ammonium persulfate (APS), Tetra (ethylene glycol) diacrylate (TEGDA), and Kaolinite were procured from Sigma-Aldrich (USA) and used without additional extraction. Sodium hydroxide (NaOH) Sodium Chloride (NaCl) was bought from Loba Chemicals (India). Triple distilled water was used for all preparations.

Synthesis of superabsorbent composite (SACs)

Graft copolymerization technique was used for the synthesis of superabsorbent composite (SACs) in which IA grafted on to xanthan gum polysaccharides in the company of inorganic filler kaolinite, TEGDA as an agent who works as cross-linker, and APS as an initiator to start the polymerization. In this process, xanthan gum (0.4–1.9 g) in 250 ml reactor was added with 40 ml distilled water and degassed for half an hour.

The reactor was placed at 70 °C in a water bath. Kaolinite powder (1.85–0.20 g) was added into the reactor when xanthan gum completely dissolved and stirred for 30 min at 250 RPM. Then, the calculated amount of completely neutralized itaconic acid and TEGDA (0.04–0.1 g) were added into the reactor. After a desirable time, the APS initiator (0.04–0.3 g) was added into the reactor. The polymerization was preceded for 2 h in an inert atmosphere with continuous stirring at 500 RPM. During the over of the propagation step, viscous gel products were formed and the reaction terminates with the introduction of oxygen into the reactor and the termination step started. The product was poured in water–methanol mixture (1:3) ratio, filtered, and placed into an oven at 100 °C for 48 h. The superabsorbent composite was ground, kept away from light, heat, and moisture. The particle size of superabsorbent composite 40–60 mesh in the range. Grafting ratio (%G) is calculated according to Fanta's definition [39].

$$\text{Grafting percentage } (G\%) = \frac{\text{XG-}g\text{-PIA}}{\text{XG}} \times 100 \tag{1}$$

where XG-*g*-PIA and XG represent superabsorbent composite (SACs) and xanthan gum, respectively.

The mechanism of polymerization and crosslinking reaction Scheme 2 planned and various reactions are given as follows.

Characterization

Infrared spectra (IR) were taken on a Bruker FT-IR spectrometer (Vector 33) using highly pure potassium bromide. SEM (Hitachi S-5200) was used to detect the cross-section morphology of the superabsorbent composites (SACs).

Measurement of swelling

A calculated amount of 46–60 mesh superabsorbent composite was added into 220 mesh acrylic gauge normally known as Tea Bag used for the measurement [40, 41]. The gauge was immersed in 200 ml of saline solution (i.e., 0.9 weight percent sodium chloride). After 30 min, the gunge in which superabsorbent composite was present was taken out from the solution and hanged for 30 min in the air so that the excess amount of NaCl filtered by the process of natural gravity. So that the weight of the swollen ratio of SACs was calculated by the following equation. The free water absorbency calculated in terms of equilibrated swelling (Q_{eq}) was given by the equation:

$$Q_{eq} = \frac{M_s}{M_d} - 1 \tag{2}$$

The water holding capacity of SACs

The permeability was calculated 3.5 times as gm. of H_2O per gm of dehydrated super absorbent composites (g/g). The precision of the extents was 64%. The

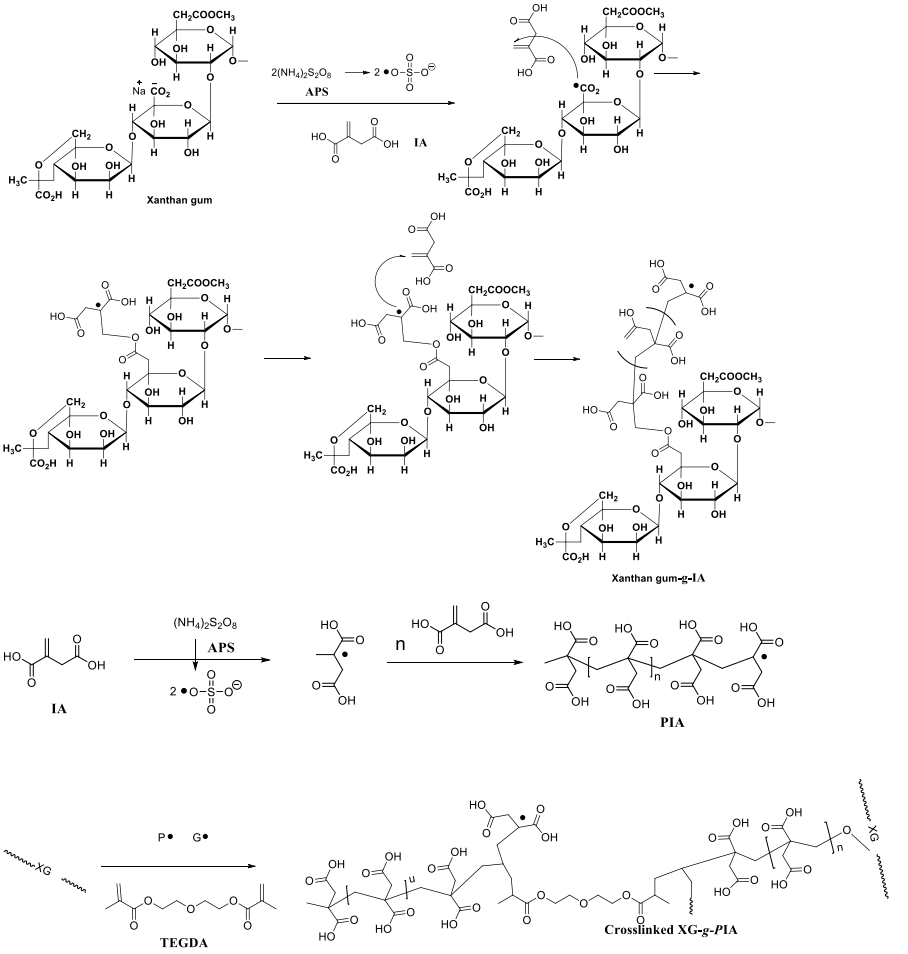

Scheme 2 Mechanism of polymerization and crosslinking reactions

standard deviation (S.D.) is calculated by the equation given below for sample data of limited size

$$\text{S.D.} = \left(\frac{\sum_{i=1}^{N} Y_i - \overline{Y}}{N-1} \right)^{1/2} \tag{3}$$

where $Y_i - \overline{Y}$ is the deviation from the usual of ith extents and N is the number of duplicates of each extent ($N = 3.5$).

The extent of absorbency under load (AUL)

For the proposes of investigation of permeability under load, a porous sintered glass filter plate ($d=80$ mm, porosity # 0, $h=7$ mm) was sited in a glass dish (Petri) ($h=14$ mm, $d=120$ mm); dried calculated amount (0.2 ± 0.02 g) of superabsorbent composite SACs was spread on acrylic gauge placed on the sintered glass. A cylinder-shaped dense mass (Teflon, $d=70$ mm, flexible height) which might be slip-up easily in a glass tube ($d=60$ mm, $h=50$ mm) was used to apply the preferred load (applied load 0.2, 0.5, or 0.8 Psi) to the dehydrated superabsorbent composite SACs as shown in Fig. 1. All gathering was fixed and kept in a gutter enclosing 0.8 weight present NaCl in such technique that solution height beyond the thickness of SAPs. The swelling proportion underweight was measured retro for a given weight at ambient temperature. The following equation is used for the AUL calculation [42–44].

$$\mathrm{AUL}_{g/g} = \frac{M_1}{M_0} - 1 \tag{3}$$

where M_1 swollen gel weight (under load) and M_0 is polymer dry weight.

Proof of grafting

The superabsorbent polymer Xanthan gum-*g*-itaconic acid is prepared by the copolymerization process represented by FTIR spectra in Fig. 2. The peak changes to 3315 cm^{-1} shifted to 3354 cm^{-1} when compared with polysaccharides xanthan gum spectra due to its assigned OH widening vibration of XG. FTIR of Xanthan gum [35] and XG-*g*-PIA on comparing at 3315 cm^{-1}, due to the OH

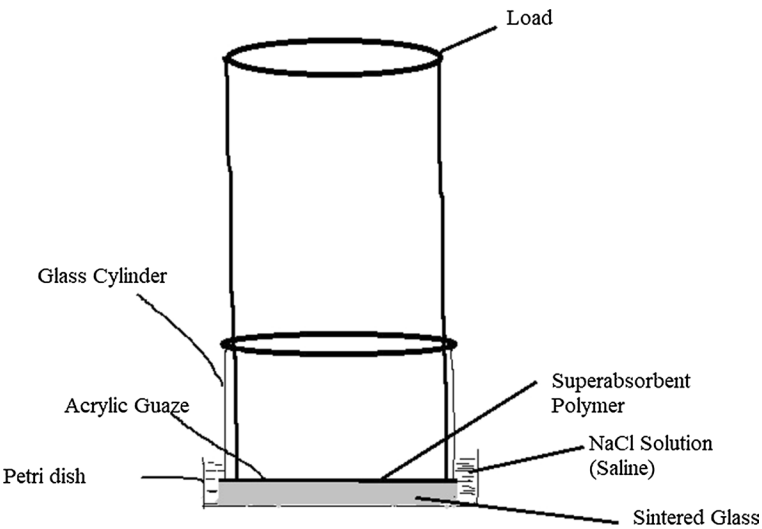

Fig. 1 Absorbency under load (AUL) tester

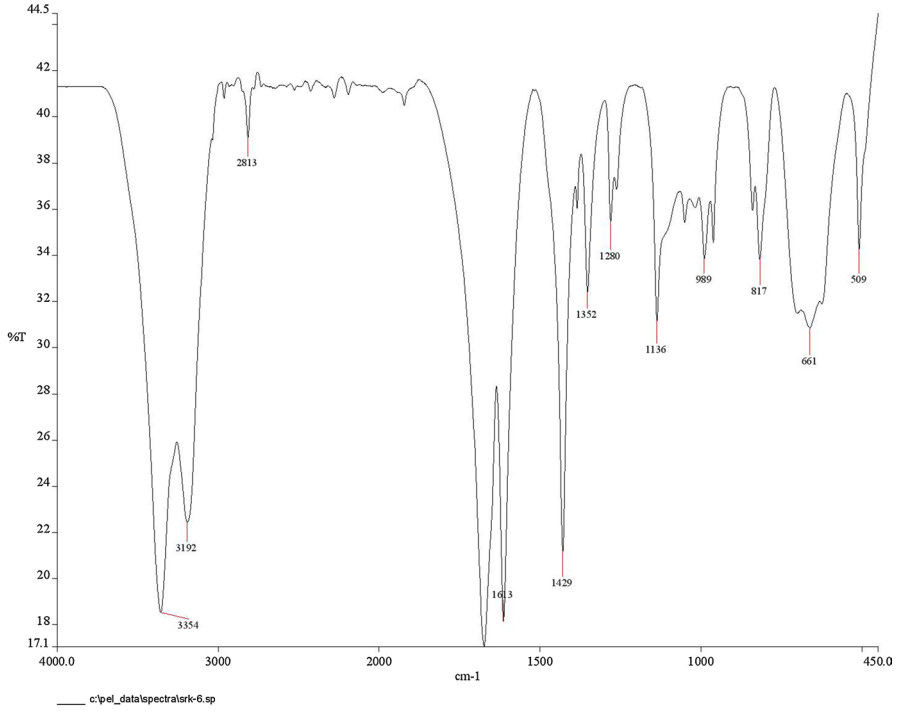

Fig. 2 FTIR spectrum of XG-*g*-PIA

widening vibration of XG, shows dropping strength involved in polymeric reactions. The band peak 2955 cm^{-1} for C–H (stretching) and 1610 cm^{-1}widening to angular distortion of the CΞC stretching is further confirmed the polymerization. The band peak was assigned at 1432 cm^{-1} accredited to CN bond widening with an average strength peak at 720–670 cm^{-1} attributed to NH flapping vibration. The FTIR spectrum was in decent contract with the proposed structure as represented in Scheme 2.

The ester group formed during the polymerization and represented by absorption peak 1719 cm^{-1}. The OH-groups associated kaolinite interacts with di-carboxylate groups of the poly (itaconic acid) give rise in the formation ester represented by Scheme 3.

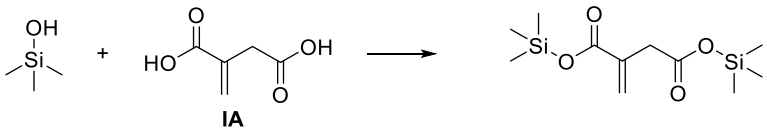

Scheme 3 Ester formation in Kaolinite surface

Scanning electron microscopy (SEM)

XG and GG-*g*-IA morphology was examined by SEM analysis represented native Xanthan gum (Fig. 3a) molded with round structures but superabsorbent polymer exhibited that (XG-*g*-PIA) composite superabsorbent shows a, respectively, free, uneven, and rippling surface produced by presenting kaolinite rough formed (dump) assemblies which were originated due to PIA/kaolinite incorporated as represented in Fig. 3b

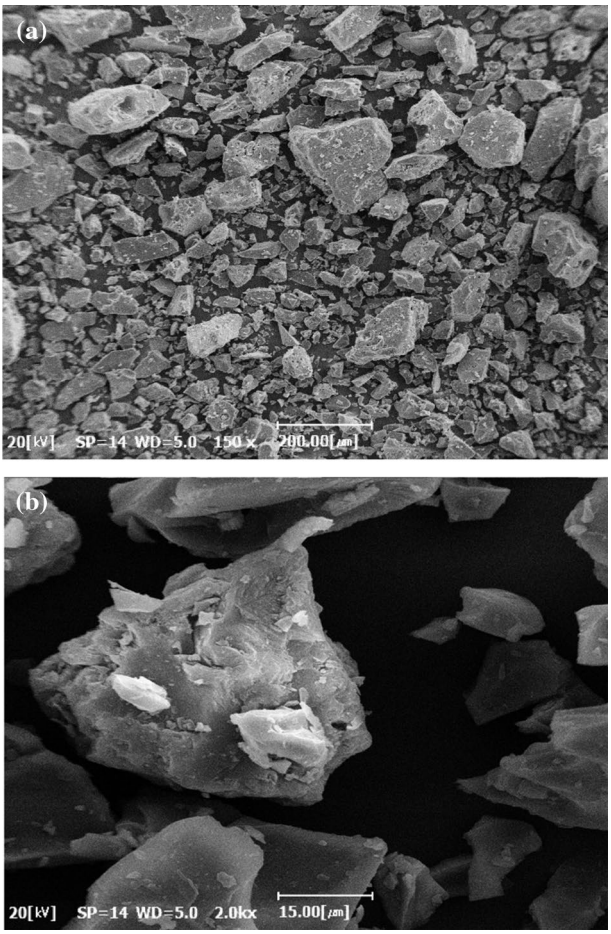

Fig. 3 **a** SEM image of the cross-section morphology of Xanthan gum, **b** SEM image of cross-section morphology of SAPs

Optimization of solution polymerization

Effect of initiator concentration

The initiator (APS) concentration effects on polymeric reaction and holding capacity of water were studied by a change in concentration ranges between 0.1 and 1.5 weight present (Figure-S1). With changing concentration from 0.1 to 1.0 wt% losses with an additional rise in the quantity of APS. It is clear that in polymerization especially free radical using a chemical initiator APS, the molecular weight in the polymerization will drop with the rise of the APS concentration. An additional reason for decreases of the molecular weight is that the comparative quantity of polymeric sequence finishes rises at great levels of APS amount. Since molecular weight contrariwise depends on initiator concentration lower molecular weight (MW) in turns to be a lower grafting present of the polymeric sequence ends do not participate in the water absorbency. There is a decrease in the holding capacity of water with the rise of the initiator APS attentiveness. A decrease in KPS content attended a decrease in absorbency due to a reduction in the number of radicals formed as the concentration of APS falls.

An additional reason, according to Flory, is the imperfection of polymer networks obtained from high-initiator polymerization systems. The increase in the number of active sites on the XG led to an increase in poly (IA) grafting onto XG backbones. There is a decrease in water absorbency with initiator concentration beyond 0.5 wt. The percent may be due to: (a) an increased number of radicals led to termination by bimolecular collision, (b) a predominance of homopolymerization over grafting, (c) molecular weight loss of the synthetic part of the polymer network, and (d) free radical degradation of XG substrate. A similar observation in the case of the degradation of chitosan with potassium persulfate has been recently reported [45].

Effect of degree of neutralization (Dn)

The significance of the degree of neutralization of itaconic acid on the holding capacity of water is represented in Figure-S2. As the neutralization degree of IA increases, water absorbency rises from 40 to 60%. This fall in water absorbency may be due to the gripping effect between groups (carboxylate and carboxylic) acid that is greater to each group. This reason is explained by Scheme 4 in which the naturalization process to understand the polymerization mechanism. Two carboxyl groups with different pKa (4 and 6) as reported earlier [46, 47] –COOH groups, designated by A and B in the scheme. During the neutralization of IA, A group (–COOH) is near to =bond conjugative effect following and another B carboxyl group in which CH_2 worked as electron-donating represented. During the process, PKa of A at 4 and severance of A arises which leads understanding of neutralization degree on the polymerization process.

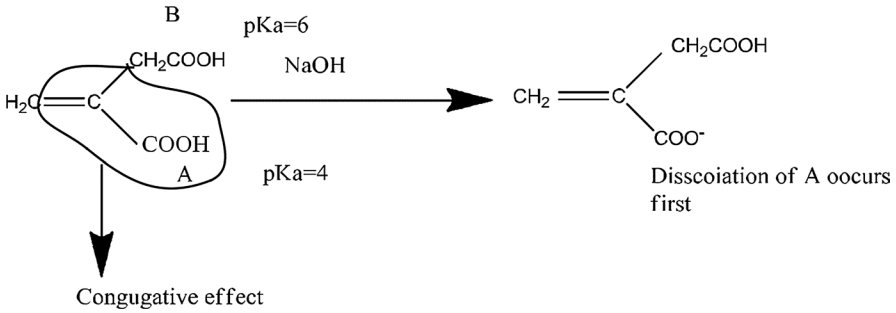

Scheme 4 Mechanism of partial neutralization of Itaconic acid monomer

It was observed that during the process of naturalization 50–70% due to the above explanation based on decarboxylation [48, 49] and radical shifted to the $–CH_2–$ group and breed another radical –COOH group as shown in the figure.

Effect of kaolinite concentration

Influence of the quantity of kaolinite on the holding capacity of water observed that tendency suddenly increases with an increasing amount of kaolinite in weight between 0 and 10% in the feed. Above 10%, kaolinite concentration the water absorbency falls with the increase in the quantity of kaolinite. As compared with XG-*g*-*P*IA superabsorbent, the H_2O absorbency of the SAP composites is greatly enhanced by the outline of kaolinite into the XG-*g*-PIA polymer network. Even when the kaolinite amount reaches 40%, the H_2O absorbency of the superabsorbent composite is greater than that of XG-*g*-PIA superabsorbent and reaches more than 1250 g/g, which significantly reduces the costs of preparing superabsorbent. Two possibilities would responsible for the special effects of kaolinite in the composite. This increase in water absorbency may effective crosslinking density decreased by introducing the kaolinite in a network of *P*IA. In the XG-*g*-PIA network, the COOH groups bounded on *P*IA chains can interact with hydrogen bonding which causes an increase in crosslinking density and gives a more tight network. While in the XG-*g*-PIA network due to the development of H_2 bonds and excess of kaolinite particles holds with the carboxylic group. This may be explained by Flory's network theory, which shows that high water absorbency lead by the low crosslinking density of the superabsorbent. The structures of kaolinite and *P*IA/ kaolinite in water is represented by schematic illustrations as shown in Scheme 5

Estimation of AUL

The holding capacity of water of SAPs changes due to peripheral circumstances such as applied pressure, swelling medium, etc. Later absorbency under load was sensibly changed in quantity to strength to the gel, absorbency under load can be measured as the gelling power of superabsorbent polymers and adult diapers [50, 51]. 200 min suitable time for attaining the maximum absorbency for various SAPs.

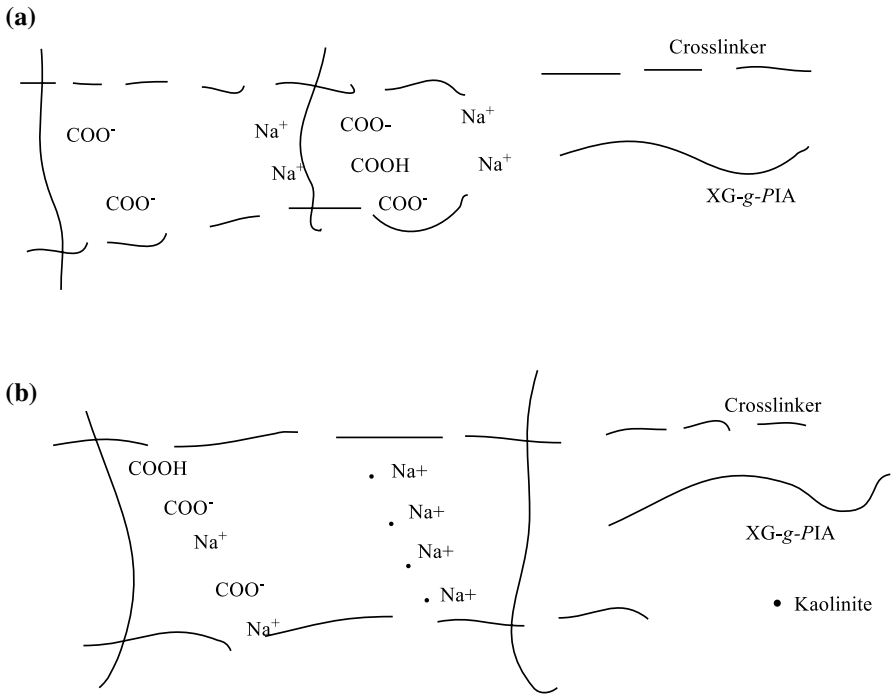

Scheme 5 Graphic illustrations of **a** *P*IA, **b** *P*IA/kaolinite structure in water

The AUL values are unaffected above this time Behavior of the SAPs swollen in 0.9 weight percent NaCl with pressure 7200 Pa measured. The applied load and swelling relation graph were plotted as the rise of the graph which helps in calculation of enlargement pressure constant and found to be 0.6% Pa as represented in Figure-S3.

Effect of Tetra (ethylene glycol) diacrylate

Figure-S4 represents the influence of TEGDA with a varying amount. Polymerization yield in this case observed to be more than 85%. In the previous study [52], superabsorbent not showed good permanence but using low TEGDA content we got a high holding capacity of water. On the increasing amount of TEGDA lesser the space among polymers units subsequently, the extremely cross-linked unbending arrangement cannot be expanded to grip a large water amount [53].

Effect of xanthan gum concentration on Water absorbency

On the varying amount of XG between 0.7 and 1.7 g dm^{-3} on water absorbency showed in Figure-S5 and decease with an increase as the amount of XG due to change in medium viscosity limits the monomer accessibility and increase the polymer unit which decreases in holding capacity of water.

Conclusion

In this study, we have shown that superabsorbent polymer composites (XG-*g*-PIA) have been synthesized through radical polymerization in aqueous medium at 65 °C in the company of ammonium persulfate and Tetra (ethylene glycol) diacrylate (TEGDA) as initiators and crosslinkers, separately and studied theirs effects on polymerization. High water absorption levels were obtained with the variation of the degree of neutralization (75%) on IA. 615.72 and 43.2 g/g swelling obtained in prepared superabsorbent. The FTIR and SEM images confirmed the synthesis of proposed SAPs. The optimized condition such as 0.2 g dm^{-3}, 0.016 mol/L, 0.02 mol/L for XG, APS, and TEGDA, respectively. Unique SAPs, the holding capacity of water was enhanced and the manufacturing cost was significantly reduced in comparison with cross-linked XG-*g*-PIA SACs. Highly absorbent polymer polymers are modified by incorporating an inorganic material to improve the swollen gel strength and to minimize the cost of the product. The results indicate that the superabsorbent polymers have relatively good potential to hold water and saline solutions both as values of the load-free absorbency (free swelling) and as values of AUL. The highly absorbent polymer absorbing water and aqueous retention may prove particularly practical in diapers and sanitary napkin uses.

References

1. Liu J, Li Q, Su Y, Yue Q, Gao B, Wang R (2013) Synthesis of wheat straw cellulose-*g*-poly (potassium acrylate)/PVA semi-IPNs superabsorbent resin. Carbohydr Polym 94:539–546
2. Park TG (1999) Temperature modulated protein release from ph/temperature-sensitive hydrogels. Biomaterials 20:517–521
3. Qiu Y, Park K (2001) Environment-sensitive hydrogels for drug delivery. Adv Drug Delivery Rev 53:321–339
4. Li A, Wang A, Chen JM (2004) Studies on poly(acrylic acid)/attapulgite superabsorbent composite. I. Synthesis and characterization. J Appl Polym Sci 92(3):1596–1603
5. Zhou WJ, Yao KJ, Kurth MJ (1996) Synthesis and swelling properties of the copolymer of acrylamide with anionic monomers. J Appl Polym Sci 62:911–915
6. Yao KJ, Zhou WJ (1994) Synthesis and water absorbency of the copolymer of acrylamide with anionic monomers. J Appl Polym Sci 53:1533–1538
7. Tsubakimoto T, Shimomura T, Kobabyashi H (1987) Jpn Pat 62:149–335
8. Holtz JH, Asher SA (1997) Polymerized colloidal crystal hydrogel films as intelligent chemical sensing materials. Nature 389:829–832
9. Adhikari B, Majumdar S (2004) Polymers in sensor applications. Prog Polym Sci 29:699–766
10. Tanaka H, Kambayashi T, Sugiyama Y, Nagai T, Nagata K, Kubota K, Hirano K (1992) Eur Pat 501:482
11. Walker CO (1987) U.S. Pat. 4: 664–816
12. Lee WF, Lin GH (2001) Superabsorbent polymeric materials VIII: Swelling behavior of crosslinked poly [sodium acrylate-co-trimethylmethacryloyloxyethyl ammonium iodide in aqueous salt solutions. J Appl Polym Sci 79:1665–1674
13. Lee WF, Yang LG (2004) Superabsorbent polymeric materials XII. Effect of montmorillonite on water absorbency for poly[sodium acrylate] and montmorilonite nano composite superabsorbent. J Appl Polym Sci 92:3422–3429
14. Kabiri K, Zohuriaan-Mehr MJ (2004) Porous superabsorbent hydrogel composites: synthesis, morphology and swelling rate. Macromol Mater Eng 289:653

15. Li A, Wang A (2005) Synthesis and properties of clay-based superabsorbent composite. Eur Polym J 41:1630–1637
16. Wang WA, Zhang J, Chen H, Wang A (2005) Study on superabsorbent composite. VIII. Composite based on acidified attapulgite and organo-attapulgite. Eur Polym J 41:2434–2442
17. Pourjavadi A, Mahdavinia GR (2006) Chitosan-*g*-poly (acrylic acid)/kaolin superabsorbent composite: synthesis and characterization. Polym Polym Compos 14:203–211
18. Wu JH, Wei YL, Lin JM, Lin SB (2003) Study on starch-graft-acrylamide-mineral powder superabsorbent. Polymer 44:6513–6520
19. Lin J, Wu J, Yang Z, Pu M (2001) Synthesis and properties of poly(acrylic acid)/mica superabsorbent nanocomposite. Macromol Rapid Commun 22:422–424
20. Lee WF, Chen YC (2005) Effect of intercalated reactive mica on water absorbency for [sodium acrylate] composite superabsorbent. Eur Polym J 41:1605–1612
21. Santiago F, Mucientes AE, Osorio M, Rivera C (2007) Preparation of composites and nanocomposites based on bentonite and poly(sodium acrylate). Effect of amount of bentonite on the swelling behaviour. Eur Polym J 43:1–9
22. Wu J, Lin J, Zhou M, Wei C (2000) Synthesis and properties of starch-*graft* -polyacrylamide/clay superabsorbent composite. Macromol Rapid Commun 21:1032–1034
23. Gao D, Heimann RB, Lerchner J, Seidel J, Wolf G (2001) Development of a novel moisture sensor based on superabsorbent poly(acrylamide)-montmorillonite composite hydrogels. J MaterSci 36:4567–4571
24. Zhang J, Li A, Wang A (2006) Study on absorbent composite. VI. Preparation, characterization, and swelling behavior of starch phosphate-graft-acrylamide-attapulgite superabsorbent composite. Carbohydr Polym 65:150–158
25. Ajabshira SZ, Niasaria MS, Ajabshirb ZZ (2016) $Nd_2Zr_2O_7$–Nd_2O_3 nanocomposites: new facile synthesis, characterization and investigation of photocatalytic behavior. Mater Lett 180:27–30
26. Morassaei MS, Ajabshira SZ, Niasaria MS (2016) Simple salt-assisted combustion synthesis of Nd_2Sn_2O7–SnO_2 nanocomposites with different amino acids as fuel: an efficient photocatalyst for the degradation of methyl orange dye. J Mater Sci Mater Electron 27:11698–11706
27. Ajabshira SZ, Niasaria MS, Ajabshirb ZZB, Bagheri S, Hamid SBA (2017) Facile preparation of $Nd_2Zr^2O_7$–ZrO_2 nanocomposites as an effective photocatalyst via a new route. J Energy Chem 26:315–323
28. Razi F, Ajabshira SZ, Niasaria MS (2017) Preparation, characterization and photocatalytic properties of Ag_2ZnI_4/AgI nanocomposites via a new simple hydrothermal approach. J Mol Liq 225:645–651
29. Ajabshira SZ, Morassaei MS, Niasaria MS (2019) Eco-friendly synthesis of Nd2Sn2O7-based nanostructure materials using grape juice as green fuel as photocatalyst for the degradation of erythrosine. Compos Part B 167:643–653
30. Ajabshira SZ, Niasaria MS (2019) Preparation of magnetically retrievable $CoFe_2O_4$@SiO_2@$Dy_2Ce_2O_7$ nanocomposites as novel photocatalyst for highly efficient degradation of organic contaminants. Compos B 174:106930
31. Ajabshira SZ, Morassaei MS, Niasaria MS (2019) Facile synthesis of $Nd_2Sn_2O_7$–nO_2 nanostructures by novel and environment-friendly approach for the photodegradation and removal of organic pollutants in water. J Environ Manag 233:107–119
32. Ajabshira SZ, Derazkola SM, Niasaria MS (2018) Nd_2O_3–SiO_2 nanocomposites: a simple sonochemical preparation, characterization and photocatalytic activity. Ultrason Sonochem 42:171–182
33. Ajabshira SZ, Derazkola SM, Niasaria MS (2017) Simple sonochemical synthesis of Ho_2O_3–SiO_2 nanocomposites as an effective photocatalyst for degradation and removal of organic contaminant. Ultrason Sonochem 39:452–460
34. Morassaei MS, Ajabshir SZ, Niasaria MS (2016) New facile synthesis, structural and photocatalytic studies of NdOCl–$Nd_2Sn_2O_7$–SnO_2 nanocomposites. J Molec Liq 220:902–909
35. Jeong G, Bak J, Yoo B (2019) Physical and rheological properties of xanthan gum agglomerated in fluidized bed: effect of HPMC as a binder. Int J Biol Macromol 121:424–428
36. Maiti S, Ray S, Sa B (2008) Effect of formulation variables on entrapment efficiency and release characteristics of bovine serum albumin from carboxymethyl xanthan microparticles. Polym Adv Technol 19(7):922–927
37. Sand A, Vyas A (2020) Superabsorbent polymer based on guar gum-graft-acrylamide: synthesis and characterization. J Polym Rese 27:1–10

38. Sand A, Vyas A, Gupta AK (2016) Graft copolymer based on (sodium alginate-g-acrylamide): Characterization and study of Water swelling capacity, metal ion sorption, flocculation and resistance to biodegradability Intern. J Bio Macrom 90:37–42
39. Fanta GF (1973) Block and graft copolymerization. In: Ceresa RJ (ed) Wiley, New York, p 1
40. Bao Y, Ma J, Li N (2011) Synthesis and swelling behaviour of sodium carboxy methyl cellulose-*g*-poly[AA-co-AM-Co-AMPS]-montmorilonite superabsorbent hydrogel. Carbohydr Polym 84:76–82
41. Bruna J, Yazdani-Pedram M, Quijada R, Valentín JL, Lopez-Manchado MA (2005) Melt grafting of itaconic acid and its derivatives onto an ethylene-propylene copolymer. React Funct Polym 64:169–178
42. Ma S, Liu M (2004) Preparation and properties of a salt-resistant superabsorbent polymer. J Appl Polym Sci 93:2532–2541
43. Doo-Won L, Kee-Jong Y, Sohk-Won KO (2000) Synthesis of AA-based superabsorbent interpenetrated with sodium PVA sulfate. J Appl Polym Sci 78:2525–2532
44. Khare AR, Peppas NA, Massimo G, Colombo P (1992) Measurement of the swelling force in ionic polymer networks: I. Effect of pH and ionic content. J Control Release 22:239–244
45. Sand A, Yadav M, Behari K (2010a) Graft copolymerization of 2-acrylamidoglycolic acid on to xanthan gum and study of its physicochemical properties. Carbohydr Polym 81:626–632
46. Yazdani-Pedram M, Vega H, Quijada R (2001) Melt functionalization of polypropylene with methyl esters of itaconic acid. Polymer 42:4751–4758
47. Sand A, Yadav M, Behari K (2010b) Preparation and characterization of modified sodium carboxymethyl cellulose via free radical graft copolymerization of vinyl sulfonic acid in aqueous media. Carbohydr Polym 81:97–103
48. Li J, Brill TB (2001) Spectroscopy of hydrothermal solutions 18: pH-dependent kinetics of itaconic acid reactions in real time. J Phys Chem A 105:10839–10845
49. Ramazani-Harandi MJ, Zohuriaan-Mehr MJ, Yousefi AA, Ershad-Langroudi A, Kabiri K (2006) Rheological determination of the swollen gel strength of superabsorbent polymer hydrogels. Polym Test 25:470–474
50. Ma S, Liu M, Chen Z (2004) Preparation and properties of a salt-resistant superabsorbent polymer. J Appl Polym Sci 93:2532–2541
51. Siepmann J, Peppas NA (2001) Modelling of drug release from delivery system based on hydroxyl propyl methyl cellulose (HPMC). Adv Drug Deliv Rev 48:139–157
52. Sugama T, Cook M (2000) Poly(itaconic acid)-modified chitosan coatings for mitigating corrosion of aluminum substrates. Prog Org Coat 38:79–87
53. Sand A, Yadav M, Mishra DK, Behari K (2010) Modification of alginate by grafting of *N*-vinyl-2-pyrrolidone and studies of physicochemical properties in terms of swelling capacity, metal-ion uptake and flocculation. Carbohydr Polym 80:1147–1154